Title

Evaluation and systematic selection of significant multi-scale surface roughness parameters (SRPs) as process monitoring index

Authors

Das, Jayanti
Linke, Barbara

Publication Date

2017-06-01

DOI

10.1016/j.jmatprotec.2017.01.017

Peer reviewed

Evaluation and systematic selection of significant multi-scale surface roughness parameters (SRPs) as process monitoring index

Jayanti Das[a], Barbara Linke[a*]

University of California, One Shields Ave, Davis 95616, CA, USA

*Corresponding author. Tel.: +1-530-752-6451; *E-mail address:* bslinke@ucdavis.edu

Abstract

The evaluation of multi-scale surface roughness parameters (SRPs) is important to solve many engineering problems (e.g. contact stress, sealing, friction) and is closely related to further fundamental problems (e.g. microbial contamination). Traditionally, surface roughness has been used as a standard for indicating process performance, such as tool wear, tool vibration etc. This paper also aims to find appropriate surface roughness parameters (SRPs) that can be used as process monitoring indices. Grade 304 stainless steel surfaces, generated by extrusion and grinding processes, were used in this study. The evaluation of different SRPs and their topography properties (such as fractal dimension) is discussed for extruded and ground surfaces. One problem with existing surface metrology is the availability of a multitude of disconnected roughness parameters. A statistical approach is presented in this paper that allows the most appropriate roughness parameters to monitor whether the intended surface quality converges to be found.

Keywords: Surface roughness, fractal dimension, finishing process, surface functionality, surface texture

Nomenclature

Average Roughness	Ra, Sa
Core Roughness Parameters	Rk, Sk
Cross Correlation	r
Fractal Dimension	Ds
Kurtosis	Rku, Sku
Material Ratio	Smr_1, Smr_2
Maximum Peak Height	Rp, Sp
Mean Value	μ
Number of Samples	n
Reduced Peak Height	Rpk, Spk
Root Mean Square Deviation of Profile	Rq, Sq
Skewness	Rsk, Ssk
Solidity Ratio	K
Standard Deviation	σ
Total Height of Profile	Rt, St
t-test	t
Valley Depth	Rvk, Svk

1. Introduction

Finding the right balance between reliable product performances and maximizing manufacturing process efficiency is complex and depends on a large number of processing factors. Different tool geometries, choice of cutting tools and workpiece materials, tool and machine wear, processing time are some of very critical factors among a vast amount of other considering factors (Jawahir et al., 2011). Among the high volume of input output parameters, surface roughness plays a significant role for assessing product performance. Different surface roughness parameters (SRPs) not only affect the mechanical and physical properties (e.g. friction coefficient, residual stress) of mating parts, but also the optical behavior and coating behavior of non-contacting parts like shininess or glossiness (Linke and Das, 2016). Thus, surface roughness parameters can control the surface functional properties like wear, friction, lubrication, fatigue, sealing, reflection, adhesion of microorganisms, visual and aesthetic appearance. Moreover, the surface roughness of organs, tissues, texture direction of fresh produce (i.e. lettuce, spinach) is becoming a great area of interest for biologists, food scientists, and metallurgists who seek to control persistent food outbreak over the past few years (Han et al., 2016).

Measurement and analysis of surface topography is important to all industries. Three-dimensional characterization gets more attention due to increased availability of optical, nondestructive measurement methods. Different ISO standards were established to standardize roughness parameters. (Whitehouse, 2011) and (Leach, 2013) described the physical significance of different 2D profile and 3D areal surface roughness parameters. Generally, different roughness features refer to amplitude, spatial distribution, texture direction, or pattern of surfaces (Zhou et al., 2016). Conventionally, average profile or areal roughness (i.e. Ra, Sa), average maximum height (i.e. Rz, Sz), or maximum height (Rt) of the profile are most widely used in

industries in order to evaluate surface metrological features (Terry and Brown, 1997). However, Ra, Rz, or Rt only refer to amplitude variation or extreme features of surfaces but do not assess the shape of the profile, which defines functionality like bacterial retention, microbial growth, stress, etc (Asiltürk et al., 2016). Therefore, other stratified and functional parameters, like skewness (Ssk), kurtosis (Sku), load bearing area curve (BAC), volumetric ratio, or core roughness parameter (Rk), can be more useful parameters for a detailed analysis of surfaces (Raymond et al., 2016).

The aim of this paper is to evaluate stratified and functional parameters for extruded and ground surfaces comprehensively to predict texture behavior more accurately. Since advanced manufacturing processes are more and more focusing on producing smart surfaces in a cost-effective way, the second aim of this paper is to find a systematic approach to choose a few appropriate roughness parameters that can act as process monitoring indices for different manufacturing processes.

2. Background

Abrasive finishing operations, like grinding, polishing, or lapping, work with multiple cutting edges. (Kiyak and Çakır, 2007) found that different abrasive grain sizes (given as mesh numbers) and grain size distributions change surface roughness and affect functionality. (Linke, 2015) has discussed the importance of proper selection and implementation of abrasive tools for machining. (Das and Linke, 2016) has shown how the abrasive grit numbers and process parameters are used to achieve the desired surface quality and can be used for process optimization. A simple schematic of interdependence between surface characterization, process control, and function of surface is shown in Fig. 1.

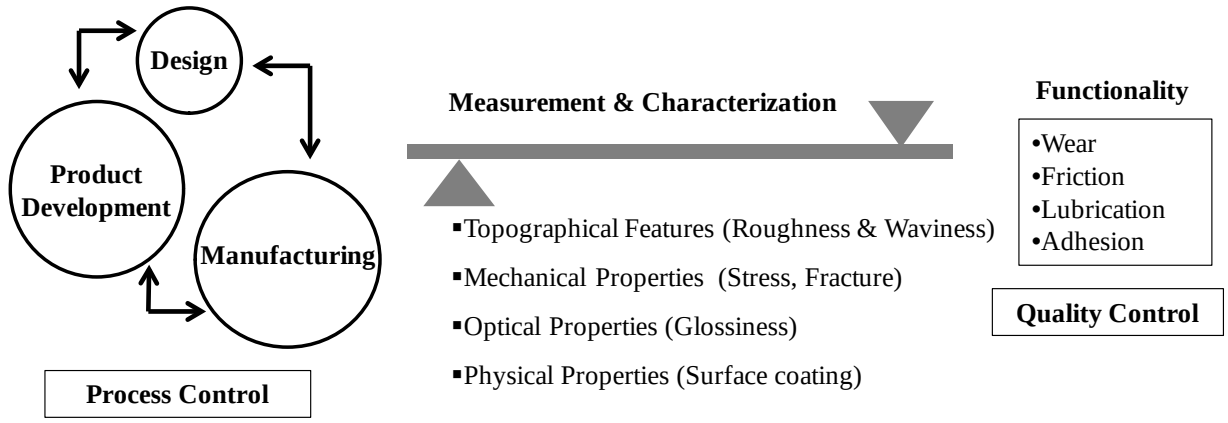

Fig. 1: Schematics of Interrelation between Process Control and Functionality

However, researchers express growing concerns about producing reliable, safe, and efficient components for automotive, aerospace, and biomedical industries. A significant number of papers evinced surface metrology as an important tool for controlling product properties like fatigue strength, resistance to corrosion, service life, etc. For example, (Javidi et al., 2008) showed the impact of cutting speed, feed rate, and tool nose radius on fatigue life of steel components during hard turning. (Seemikeri et al., 2008) presented how low plasticity burnishing (LPB) operation can stabilize surface compression properties and can improve subsurface roughness, hardness, and fatigue strength. (Asquith et al., 2007) studied the surface microstructure and phase composition of 2021-T351 aluminium alloys and showed that plasma electrolytic oxidation (PEO) can reduce corrosion at the surfaces. (Vulliez et al., 2014) showed a strong correlation between stress-relieving heat treatment and fatigue limit. However, there is not enough information available in the available literature that can comprehensively describe how to correlate surface metrology quantitatively with surface functional performance.

The root cause of the problem lies in a lack of systematic information about surface metrology and its connection to product and part design for various manufacturing processes. As a result, the majority of part drawings only focuses on information about surface finish but not on

physical, mechanical, and metallurgical properties of surfaces and their interdependencies with surface functionalities. For example, (Griffiths, 1993) described mechanical properties and characteristics for deep drilling but gave no recommendations to implement requirements in practice. (Seyeux et al., 2015) found that adherence of bacteria changes the chemical composition of passive films on stainless steel surfaces, but it is still unclear if bacterial adhesion occurs due to oxide film formation or for metallic surface roughness. (Simões et al., 2010) showed that attachment of microorganisms mostly occurred on rough, hydrophobic surfaces coated by surface conditioning films, which is basically adsorption of macro molecules on the substrate, but no recommended ranges of roughness are mentioned for industrial application. On the contrary, (Hilbert et al., 2003) showed there is no effect of surface roughness on bacterial attachment for the 316 steel surfaces in a flow system but there is a relationship with corrosion resistance. (Matsumura et al., 2013) found that wettability depends on the shape and alignment of the surface topography but did not explain how chemical coating, contact area, or density limits can influence wettability and part performance of machined products.

As mentioned before, much research work has focused on different 2D and 3D SRPs to establish correlations with relevant surface properties. For example, investigations by (Krolczyk et al., 2016) on ground and turned surfaces showed that 3D amplitude parameters, like standard deviation of profile height distribution (Sq), maximum profile peak height (Sp), maximum profile valley depth (Sv), Sz, and Sa, are strongly dependent on the manufacturing processes. They also proved that skewness and kurtosis have strong correlations with grit size in the abrasive blasting process. (Grzesik, 2016) showed that both 2D and 3D SRPs correlate with surface mechanical and chemical properties like fatigue, corrosion resistance, adhesion, and bonding strength. (Bigerelle et al., 2012) showed sharp peaks on surfaces were normally abraded

away during grinding due to cohesion, whereas round peaks are removed due to adhesion. This phenomenon also helps to predict the wear rate between two mating surfaces. (Ţălu et al., 2014) concluded that multifractal characterization could be a prospective tool to determine heterogeneity of surface texture. (Grzesik et al., 2015) showed that for the same average roughness (Sa), the surface produced by high precision machining can have completely different spatial distributions and fractal properties. (Raymond et al., 2016) investigated wear resistant properties of abrasive filament tools by analyzing different surface functional parameters. (Wang et al., 2015) showed a correlation between average roughness (Ra) and fractal dimension (D_s). (Grzesik and Żak, 2015) investigated hard turned, ground and honed surfaces and found that cavities or peaks are attributes to fluid retention ability and to wear resistance. (Wang et al., 2006) developed a mixed lubrication model for non-Gaussian rough surfaces and optimized the pattern by correcting grooves, skewness, area ratio, and load ratio. Along with experimental analysis, a theoretical model was developed by (Lavernhe et al., 2014) using multi-scale areal analysis for three axis ball-end milling for predicting tool path.

Moreover, a single roughness parameter is insufficient to analyze surface texture or recognize patterns. With increasing complexity of surface texture, it becomes difficult to characterize the surface micro topography by single conventional integral dimensions. ‘Fractal’ or ‘multifractal’ geometries are features, which can be extensively used for complex and irregular shaped surfaces (Zhang and Yue, 2016). The term ‘fractal’ was first introduced by Benoît Mandelbrot in 1960 (Mandelbrot, 1989) and over the past few decades it was adapted as an important parameter for surface texture analysis (Terry and Brown, 1997). (Grzesik and Brol, 2003) showed that fractal dimensions are tightly correlated with Ra, Rz and can be used as tools for controlling surface finish in a complex, multistage machining process.

A fractal or multifractal structure is primarily characterized by the fractal dimension (D_s) which is a non-integer value within a range of $2 \leq D_s \leq 3$. The fractal dimension is independent of all scales of roughness parameters and is used as a quantitative parameter to describe 1D, 2D or 3D surface features. $D_s=2$ depicts an ideal, smooth surface whereas $D_s=3$ means a rough surface which lodges in all available volume (Brown et al., 1996).

A number of researchers calculated fractal dimensions over the past years by different approaches like the box counting method (BCM), differential box counting method (DBCM), fractional Brownian motion method (FBMM), variogram method (VM), area motion measurement method (AMMM), isarithm method (IM), and triangular prism method (TPM) (De Chiffre et al., 2000). Each method has its own advantages and disadvantages over others. In this paper, the box-counting method as described in (Lopes and Betrouni, 2009) was used. The fractal dimension D_s was estimated by equation (1).

$$D_s = - \lim_{r \to 0} \frac{\ln N(r)}{\ln(r)}, \qquad (1)$$

In this equation, natural logarithm of N(r) denotes minimum number of boxes of size (r). Fractal dimension D_s is the slope of the natural logarithm of the box number, N, versus the negative natural logarithm of the of the box size. A large D_s value signifies that a higher number of boxes is required to encompass the surface entirely. Also, a higher D_s value leads to a more exquisite, dense, or irregularly shaped surface texture.

A major problem in surface related research is choosing significant roughness parameters that correlate to surface formation mechanisms and surface behavior in a fundamental way. In addition to that, until recent times, SRPs have been used more as an indicator for process stability but have limited usefulness as a measure of part performance. Defining inclusive roughness parameters as performance indicators might open up new windows for more

meaningful quality assessment. In addition, 3D roughness parameters are still not as widely used as 2D parameters even though they include more information about surface texture.

3. Experimental Details

3.1 Workpiece materials and surface generation

Two different types of manufacturing processes i.e. extrusion and grinding were used in this paper as a case study. Three surface types were produced out of these two manufacturing processes i.e. one type is a pristine extruded surface and the other two types are ground surfaces made with 60 grit and 400 grit abrasive sanding bands respectively. A Dremel 4000 hand held power tool and resin bonded alumina sanding bands were used for fabricating the ground surfaces. All grinding operations were run under dry cutting conditions, performed by the same subject to improve the consistency of the manually applied forces, and were repeated three times each. The forces were measured with a Kistler piezo force sensor beneath the workpiece. Details of the grinding processes are shown in table 1.

Table 1. Details of the grinding processes

Type of Workpiece Material	304 Stainless Steel
Dimension of Workpiece	12.7 mm (L), 12.7 mm (W), 12.7 mm (H)
Material Removal Rate (MRR)	2.25 mm^3/s to 2.875 mm^3/s
Rotational Cutting Tool Speed	5000 rpm
Grinding Time	1 min
Cutting Tool Type	Alumina Sanding Bands of grit 60 & grit 400
Sanding Banding Dimension	6.35 mm diameter and 6.35 mm width
Range of Total Depth Removed per Grinding Process	0.01395 mm to 0.01783 mm
Average Normal Force	~ 2 N
Average Tangential Force	~ 0.25 N
3 types of surfaces i.e. ‘Extruded Surface’ (no grinding); ‘Ground Surface using grit 60’; ‘Ground Surface using grit 400’	

3.2 Surface topography analysis

A white light interferometer confocal microscope (Zeiss CSM 700) was used for surface measurements. A 5 x 5 stitching method under 20x magnification was applied to cover a large measurement area. In general, the precision and accuracy of a measurement depends on the measurement techniques and on the measured condition. The necessity of profile or areal analysis depends on the application of the measured parts. Areal analysis captures much more of the directional nature of the surface topography compared to profile mapping. For example, Fig. 2 refers to areal and profile mapping for an object at the same measurement area. The profile measurement alone detects discrete bumps on the surface, which might come from sudden, small surface peaks or from a random, bigger inclusion. Only areal measurement can give the accurate knowledge about the feature in question; in this case, it was a random peak on the surface. In this paper, mostly 3D parameters were analyzed although some 2D parameters were also studied for a comparative assessment. 2D parameters were obtained in the perpendicular direction of machining whereas the extruded surfaces were free from lay and thus the measurement direction was independent.

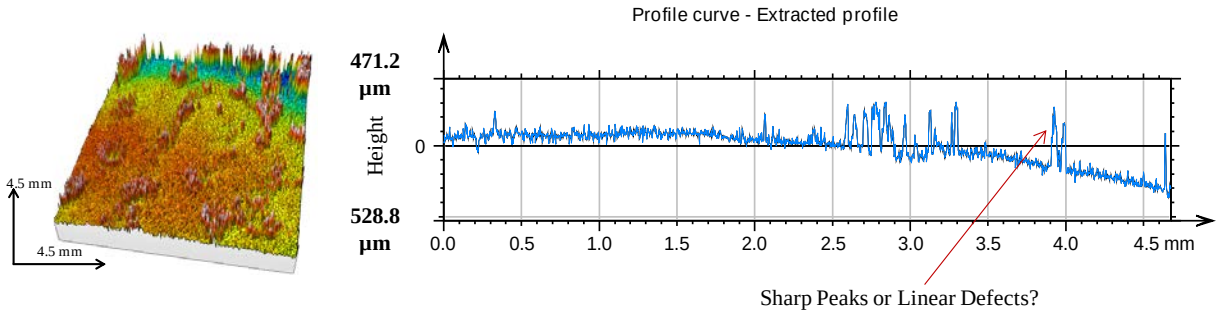

Fig. 2: Areal and Profile Analysis of Same Surface under Same Measurement Length

4. Experimental Results & Discussion

The confocal images of extruded and ground surfaces using areal and profile analyses are shown in Fig. 3. It is obvious that the extruded surface contains a large number of grooves and pits throughout the surface. The roughness of ground surfaces produced by #60 grit is in the same range as the extruded one. But instead of inordinate pits/grooves like on the extruded surface, it contains plowed material. Textures are denser and smoother for the ground surface with the higher grit size #400.

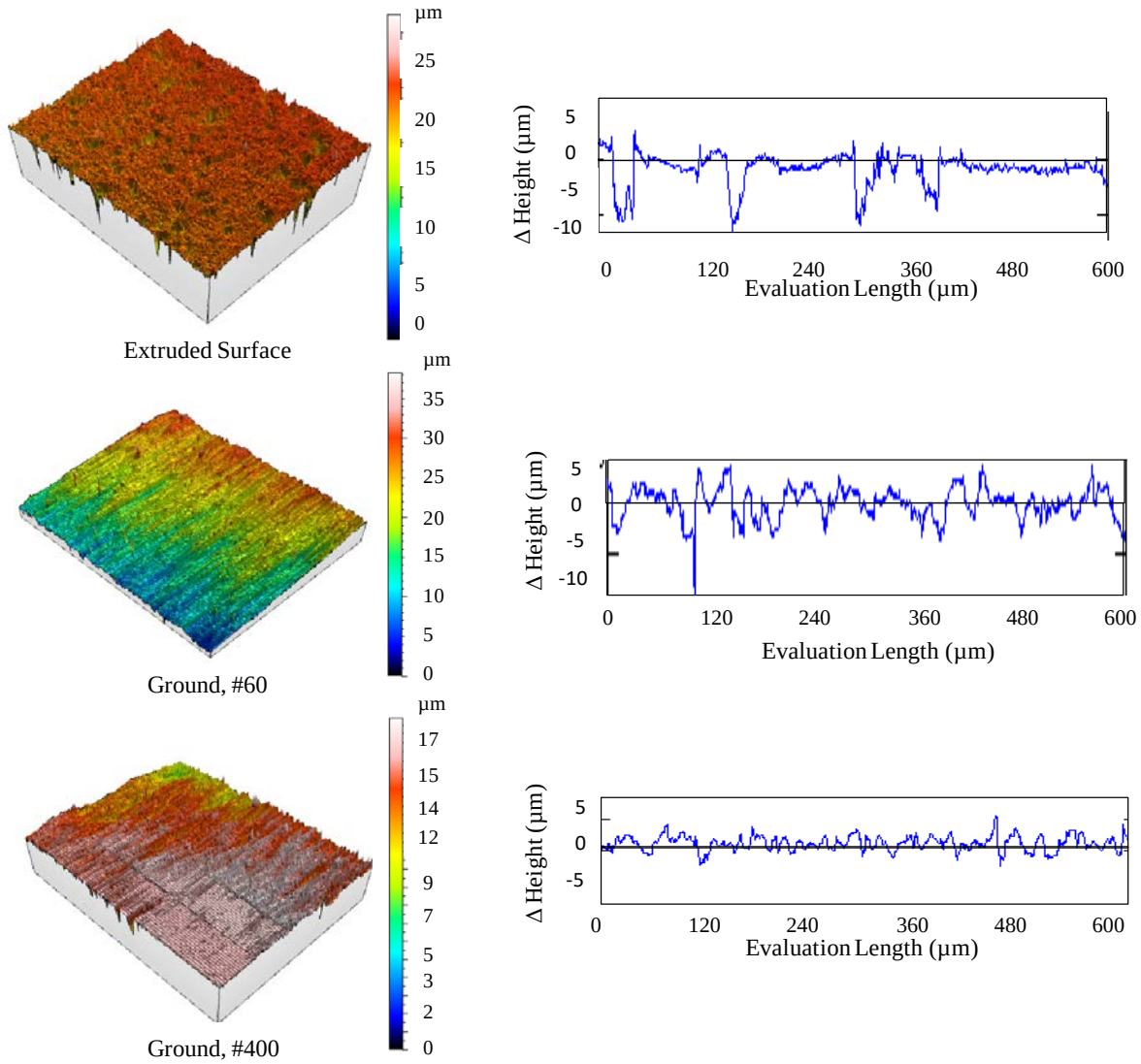

Fig. 3: 3D surface topography from 2.5 mm^2 surface area and corresponding profile lengths

Scanning electron microscopy (SEM) is a sophisticated tool used to produce images with high resolution and high depth of focus of surfaces in the micro and nanometer range. Fig. 4 shows SEM images of three different types of samples prepared for the study. The pointed arrows show pits and plowed material on the surface.

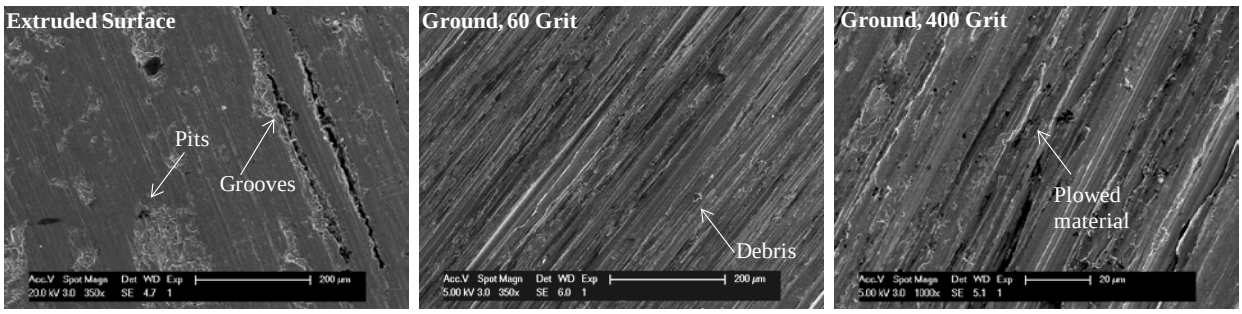

Fig. 4: Scanning electron microscopy images as examples for the studied surfaces

Since dry cutting conditions, as used in the examined grinding operations, generate excessive heat (Ebbrell et al., 2000), it is important to investigate the thermal damage and cross sectional surface layer properties after the machining process. As steps towards this, energy-dispersive X-ray spectroscopy (EDX) is used. EDX is a versatile tool offering chemical characterization of surface defects, substrate, and possible contaminations. Table 2 shows the EDX analysis of the extruded and ground samples. It indicated that only insignificant chemical changes occurred to the ground samples compared to the extruded surface.

Table 2: Energy Dispersive X-ray Spectroscopy (EDX) Element Analysis

	Si (%)	**Cr (%)**	**Fe (%)**	**Ni (%)**
Extruded Surface	0.6	18.9	72.3	8.1
Ground, #60	0.5	18.6	72.7	8.2
Ground, #400	0.8	19.1	71.7	8.4

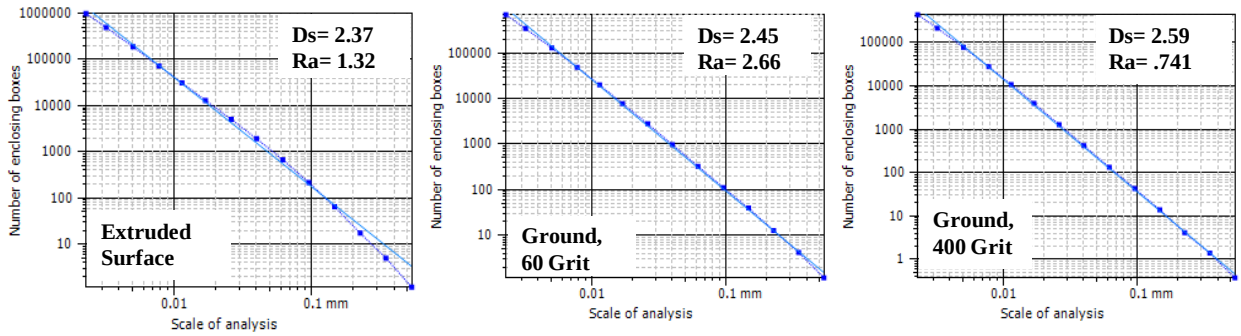

Fig. 5: Fractal Dimension Analysis for different types of surfaces

Fig. 5 shows the fractal dimension of the three different types of surfaces used in this paper and Fig. 6 shows the fractal dimensional D_s and average roughness Ra for different samples and trials. Generally, with smaller Ra, the D_s value was increased, which means texture was denser and smoother. A large number of boxes was required to lodge in the surface. For two cases out of nine cases (marked by pointed arrows in Fig. 6), small Ra were accompanied by a comparatively smaller D_s value which suggests that the surfaces contained more grooves or peaks and made the texture less dense than usual.

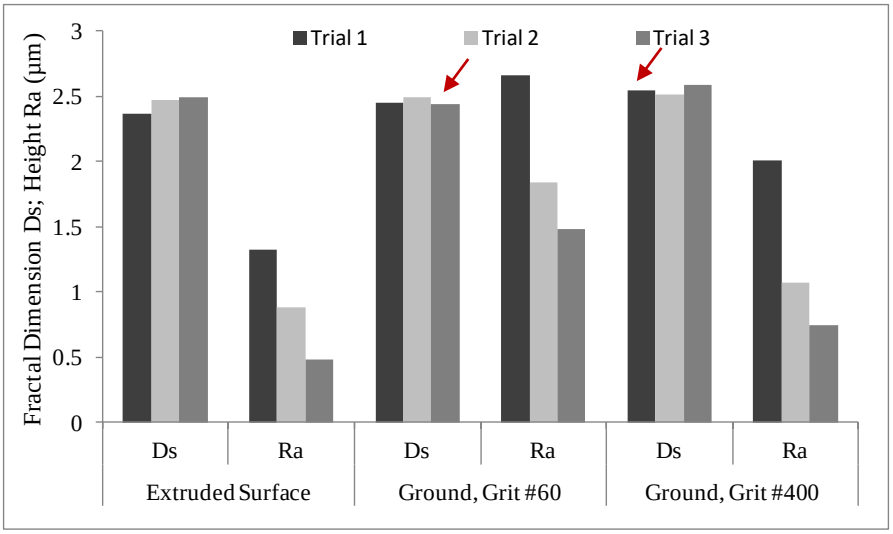

Fig. 6: Relationship between fractal dimensions with average roughness

In combination, Ra and Rq are useful to understanding any texture directionality even if these parameters are 2D profile parameters. Thus, the ratio of Ra:Rq provides information regarding

periodicity or randomness of the surface profile. A higher ratio Ra:Rq implies a higher periodicity of surface texture. For example, a sealing object, like a cylinder head gasket, requires lower roughness along the sealing direction but higher roughness along the leak path (Metrology).

High Rp implies the surface is composed of high peaks. A high ratio of Rp:Rt provides information about 'emptiness' or 'fullness'. This ratio is important for sliding contact surfaces like produced by grinding processes. A higher ratio of Rp:Rt means the surface contains a higher peak height than valley height.

The solidity ratio, K, can be defined by equation (2) (Davim, 2010):

$$K = \frac{Rt - Rp}{Rt} \qquad (2)$$

K is associated with skewness. A higher K value implies deeper grooves compared to the total height variation.

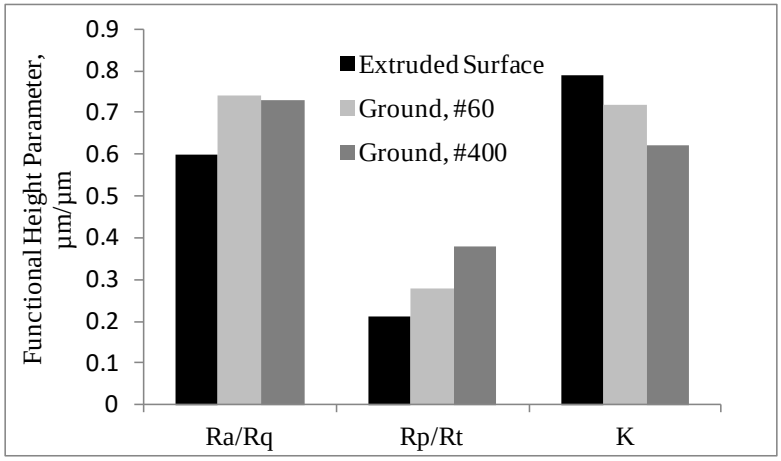

Fig. 7: Ratio of profile parameters for ground and extruded surface

Fig. 7 shows that the ground surfaces yield higher directionality (ratio Ra:Rq) compared to the extruded surfaces. The solidity ratio, K, of extruded surfaces is higher than ground surfaces, which implies that extruded surfaces subsume higher cavities. For the grinding operation with finer grits, #400, cavities were likely filled up or ground away, which improved the K value and

increased the Rp:Rt ratio. These ratios are important to study the surface 'lay' which might have a direct correlation with functionality, e.g. with bacterial retention on the surface in a certain direction.

The 3D amplitude parameters skewness (Ssk) and kurtosis (Sku) are used to evaluate surface structure, surface defects, and wear conditions. Ssk represents the peaks and valleys that are dominant on the surface. Ssk>3 signifies predominance of high peaks and Ssk<3 represents deep valleys. Kurtosis values indicate a presence of disproportionately high peaks or deep valleys (Sku>3) or lack thereof (Sku<3). Sku=3 represents an ideal Gaussian distribution of surface texture. Therefore, the combination of Sku and Ssk can pin-point the status of the surface and explain whether it contains inordinate high peaks/valleys or not.

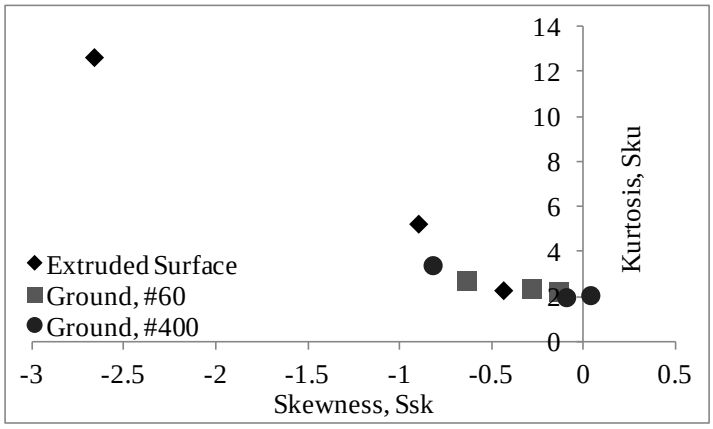

Fig. 8: Kurtosis-Skewness relationship for ground and extruded surfaces

It can be found from Fig. 8 that nearly all extruded and ground surfaces have a negative skewness (i.e. have larger plateau-like structures) but plateaus are, on average, smaller for finer abrasives. The high Sku value of the extruded surface indicates that the texture contains extreme peaks or valleys and the negative Ssk value reveals those extreme features as valleys. Overall, it can be concluded from Fig. 8 that an extruded surface has a predominance of valleys. As the

grinding continues with finer grit abrasives, the valleys are generally either removed or filled with debris from the machining process.

The 3D stratified surface parameters, i.e. Spk, Sk, Svk, Smr1, and Smr2, are described by (Whitehouse, 2011). These parameters are all derived from an areal material ratio curve based on the ISO 25178-2 standard. The Sk parameter represents the core roughness of the surface where the load will be distributed over the surface during the run-in condition (Fig. 9a). The reduced peak height (Spk) serves as the normal height distribution over the core roughness and normally decreases during finishing. The valley depth (Svk) measures depth variation under the core roughness. These valleys can entrap lubrication and debris. Here, the material ratio is the ratio of the cross sectional area of the plane at a given height of the surface over the evaluation length.

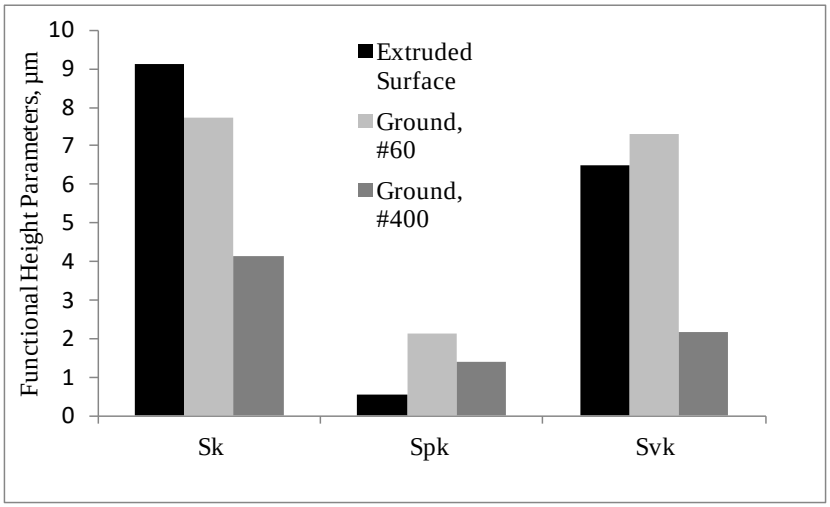

Fig. 9: Surface areal functional parameters for ground and extruded surface

Fig. 9 represents the areal functional parameters Sk, Spk, and Svk for the examined surfaces. The core roughness (Sk) of the ground surface produced by #400 is 46% lower than the 60 grit and 55% lower than the extruded surface. A lower Sk is desired for better sliding contact between contact surfaces. The surface ground with #60 sanding belt has 75% higher peaks than the extruded surface. Higher Spk values indicate an increased contact stress during sliding

performance due to the sharp-pointed, randomly distributed peaks over the surface. The ratios of $\frac{Spk}{Sk}, \frac{Svk}{Sk}, \frac{Spk}{Svk}$ values can be used to quantitatively characterize the dominance of peaks or valleys. These ratios are especially significant when two surfaces have the same conventional roughness values, for example, surfaces of sealing objects or bearings might have same average roughness but can be differentiated by the ratio Spk/Sk.

Fig. 10 shows an example of two surfaces with the same average roughness, Ra. The higher Spk/Sk ratio of the ground surfaces indicates directionality of the texture.

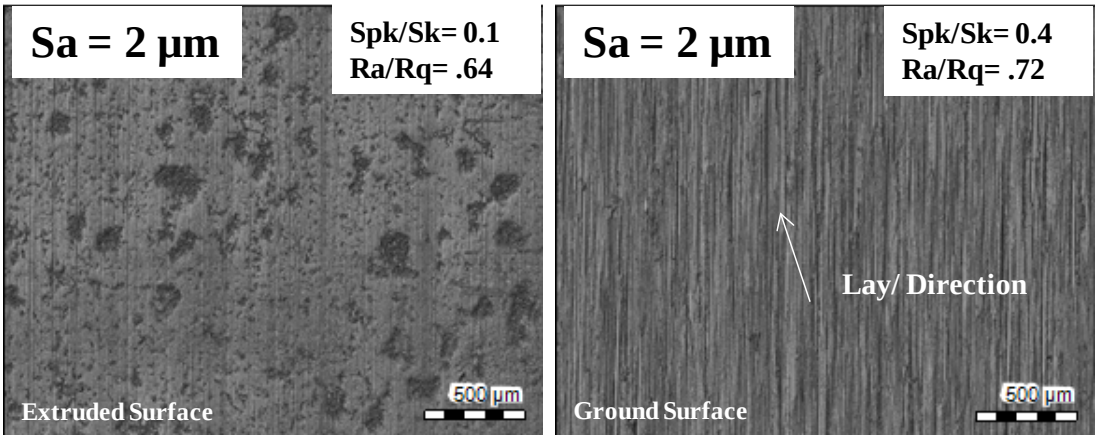

Fig. 10: Texture amplitude symmetry analysis for ground and extruded surface for same Ra

The ratios may be further insightful to analyze the texture amplitude symmetry (Metrology). Texture amplitude symmetry is a surface property, which can determine the texture amplitude distribution normalized by the overall roughness magnitude. Thus, it can potentially determine the homogeneity of surface texture. Texture amplitude symmetry has a close correlation with surface 'lay' or 'directionality' (Metrology). Higher values of the Spk/Sk ratio indicate the presence of 'lay' or certain directionalities on the surface.

Choosing Significant Roughness Parameters

Advanced and sustainable manufacturing requires efficient and cost-effective measurements and prediction of surface textures to generate functional surfaces. One shortcoming of current

metrology implementation is the limited availability of texture parameters. It is often quite difficult for a metrologist to choose the most appropriate and relevant texture parameters for monitoring whether the desired surface properties are met. The urgency of establishing a subset of surface parameters to correlate surface functionality was brought attention long ago by (Nowicki, 1985).

If a single roughness parameter has to be chosen to predict product performance, it is required to find the most significant one from the multitude of available parameters (Helmli et al., 2013). Therefore, a classification method is proposed as follows:

Three different types of surfaces, i.e. extruded and ground with two grit sizes, can be classified into three different groups i.e. group A for the extruded one, group B for the one ground with #60, group C for the one ground with #400. Two comparison studies between group A and B and between group A and C were evaluated. The average and standard deviation was calculated from three trials for each case under a 95% confidence interval as shown in Table 3.

Table 3: Average and Standard Deviation Method

	Group A extruded	Group B Ground with #60 grit	Group C Ground with #400 grit	Group A extruded	Group B Ground with #60 grit	Group C Ground with #400 grit	
	Average, μ_A	Average, μ_B	Average, μ_C	Standard Deviation, σ_A	Standard Deviation, σ_B	Standard Deviation, σ_C	P Value (95% Confidence Interval)
Sq	4.45	7.76	5.08	3.71	1.87	2.69	
Ssk	-1.33	-0.35	-0.29	1.17	0.26	0.46	
Sku	6.69	2.42	2.45	5.33	0.25	0.80	
Sp	11.01	14.83	17.13	2.32	4.32	12.16	
Sv	22.3	26.07	17.6	7.85	7.70	5.99	
Sz	33.33	40.87	34.7	8.54	4.36	16.93	
Sa	3.61	6.46	4.34	3.42	1.52	2.39	
Ds	2.44	2.46	2.55	0.06	0.026	0.04	
Sk	9.12	7.71	4.13	8.94	2.71	1.66	
Spk	0.54	2.15	1.40	0.40	0.42	0.59	
Svk	6.49	7.31	2.16	2.59	4.89	0.55	**± 2.776**
Spk/Sk	0.17	0.29	0.34	0.19	0.06	0.06	

Rp	3.96	6.53	9.14	0.88	1.78	6.43	
Rv	13.08	14.03	8.57	10.90	8.30	6.02	
Rz	17.04	20.57	17.69	11.14	10.07	12.10	
Rc	4.63	5.85	3.71	4.16	2.39	1.93	
Rt	18.83	23.43	24.2	11.47	11.54	20.26	
Ra	0.90	1.99	1.27	0.42	0.60	0.66	
Rq	1.50	2.68	1.73	0.80	1.01	0.85	
Rsk	-3.34	-0.85	0.382	1.36	0.566	1.15	
Rku	24.13	5.80	8.99	16.279	3.571082936	3.635	
Ra/Rq	0.61	0.76	0.739	0.049	0.053749418	0.06	
Rp/Rt	0.25	0.30	0.40	0.119	0.089133907	0.126	
K	0.75	0.70	0.60	0.119	0.09	0.126	

Since sample numbers are small, a simple t-test (t) was used to calculate the significance between group 'A' and 'B' or group 'A' and 'C' with equation (3). Results are shown in Table 4.

$$\text{t-test, } t = \frac{\mu_A - \mu_B}{\sqrt{\frac{((n_A-1)\sigma_A^2+(n_B-1)\sigma_B^2)}{(n_A+n_B-2)} * \frac{(n_A+n_B)}{(n_A * n_B)}}} \qquad (3)$$

Table 4: Significance between extruded & ground; and between different ground surfaces

Parameters	Significance between Extruded (A) & Ground with #60 grit (B)	Comments	Significance between Ground with #60 grit (B) & Ground with #400 grit (C)	Comments
Sq	0.090479494	significant	0.747235605	significant
Ssk	1.959048378	significant	-0.624689865	significant
Sku	-0.438260252	significant	-0.158707864	significant
Sp	0.119804497	significant	-0.04138576	significant
Sv	-0.144748616	significant	0.26690817	significant
Sz	0.011404178	significant	0.060524219	significant
Sa	0.125950903	significant	0.796935568	significant
Ds	53.76260169	Not significant	-111.4397154	Not significant
Sk	-0.181245194	significant	1.064427752	significant
Spk	5.162060441	Not significant	4.350489521	Not significant
Svk	-1.861025984	significant	0.638212296	significant

Spk/Sk	12.23146532	Not significant	-17.69412269	Not significant
Rp	0.368532676	significant	-0.175695269	significant
Rv	-0.087294059	significant	0.155797128	significant
Rz	0.007170783	significant	0.034861049	significant
Rc	-0.131054511	significant	0.68173674	significant
Rt	0.029701557	significant	-0.004229971	significant
Ra	1.860435107	significant	2.700931937	significant
Rq	0.522578193	significant	1.633489236	significant
Rsk	3.54540399	Not significant	-2.266015359	significant
Rku	-0.163435565	significant	-0.368863284	significant
Ra/Rq	72.27201136	Not significant	10.65004699	Not significant
Rp/Rt	15.29487394	Not significant	-12.00422756	Not significant
K	-15.29487394	Not significant	12.00422756	Not significant

The parameters in Table 4 with the highest significant value can be used for further classification between the two selected groups. To find the most significant roughness parameter, the calculated significance must be comparable. A simple way to do that is to use the cross correlation coefficient between two groups as followed:

$$r_{AB} = \frac{\sum_{i=1}^{n}(R_x^A - \mu^A)(R_x^B - \mu^B)}{\sqrt{\sum_{i=1}^{n}(R_x^A - \mu^A)^2 \sum_{i=1}^{n}(R_{x-}^B \mu^B)^2}} \qquad (4)$$

Here, R_x is a specific roughness parameter or ratio. The parameter that has the highest absolute cross correlation value is the most significant parameter as shown in Table 5. There are two different cases to be considered in this method:

(i) If the maximum absolute cross correlation is close to 1, then the corresponding roughness parameter can be used as a classifier.

(ii) If the maximum absolute cross correlation is close to 0, then instead of a single parameter, multiple parameters need to be used as a classifier.

Table 5: Correlation Coefficient r_{AB} for values in Table 3

	Absolute Correlation Coefficient r_{AB} between Extruded and Ground Surface (#60), r_{EG}	Comment, r_{EG}	Absolute Correlation Coefficient r_{AB} between Ground Surfaces (#60 & #400), r_{GG}	Comment, r_{GG}
	3D Parameters			
Sq	0.375267	**$r_{Sp} \approx 1$**	0.20417	**$r_{Sv} \approx \neq 0, 1$**
Ssk	0.572644		0.416958	
Sku	0.505996		0.615461	
Sp	0.994728		0.190994	
Sv	0.428657		0.634549	
Sz	0.603005		0.061779	
Sa	0.386982		0.210126	
Sk	0.239952		0.474592	
Svk	0.290032		0.517896	
	2D Parameters			
Rp	0.060703	**$r_{Rku} \approx 1$**	0.00067	**$r_{Rt} \approx 0$**
Rv	0.950225		0.104812	
Rz	0.934388		0.045335	
Rc	0.938393		0.075372	
Rt	0.900791		0.120159	
Ra	0.695025		0.092048	
Rq	0.81611		0.031142	
Rku	0.998075		0.003813	

Between extruded and ground surfaces, Sp and Rku are the most appropriate parameters to be used as a process monitoring index for 3D and 2D parameters respectively. Since the extruded surface contains a higher number of inordinate grooves, which are removed efficiently during a subsequent grinding process, the amount of peak height (Sp) or valley depth (Sz) can indicate the surface transformation best from extruded to ground. To compare between surfaces that were ground with different grit sizes, the change in valley depth is important to monitor. This is reflected in the cross-correlation results in Table 5. A low value of the cross-correlation factor (i.e. close to zero and less than 1) signifies that this single factor is less important and should only be used with other values. For example, the core roughness (Sk) is important to observe the

load bearing strength and potential contact stress but should be paired with a parameter of a higher absolute correlation coefficient.

The algorithm presented here is a very simple way to find appropriate SRPs between different groups of machined products. But if the surface texture parameters are not within disjunct confidence intervals or have multiple high significance values, it would require to choose only one for classification using other robust statistical techniques.

Conclusion

Electronics and automotive industries invest a lot of money to improve product quality for mass production. Therefore, implementing robust techniques for choosing correct selection parameters to categorize between good parts and bad parts is very advantageous for practical application. This paper describes the correlation between different surface roughness parameters with surface topographical features and presents a systematic approach to identify significant roughness parameters as a process monitoring index for manufacturing operations.

1. Overall, the extruded surface shows a lower average roughness compare to the ground surfaces, but contains inordinate large pits and grooves. This might greatly influence surface functionality like microbial contamination or fluid/debris accumulation. Grinding processes introduce plowed material on the surface but no significant chemical alteration has been observed on the surface due to heat effect induced on the workpiece.

2. Scale-area analysis is a useful tool to evaluate surface complexity. Complexity has a negative correlation with surface average roughness but shows a positive association with complex and lightly dense structures.

3. Different individual or combined surface roughness parameters (SRPs) can be directly used to describe surface topographical features. For example, the ratio Spk/Sk and the solidity ratio (K) can be used to define surface lay. Another example is the combination of skewness and kurtosis being used to define the shape of the profile to determine oil retention capacity. The $\frac{Spk}{Sk}$, $\frac{Svk}{Sk}$, $\frac{Spk}{Svk}$ ratios of areal functional parameters can be used to measure load carrying capacity or contact stress of machined surfaces.

4. A systematic selection method is useful for finding the most appropriate surface texture parameters for different manufacturing processes. Even though some parameters are significant to analyze particular surface functionalities, they might not be stable enough to be considered as process monitoring indices. Therefore, a careful and well-informed selection is suggested that takes the nature of the manufacturing operation and the desired part performance into account.

Future research should be conducted on multiple manufacturing operations and part functionalities to produce a comprehensive database. Moreover, this paper only considers amplitude and functional parameters along with scale-area analysis for surface topographical analysis. Future study should also focus on spatial parameters for detailed investigation.

Acknowledgement

The authors want to thank the Engineering Fabrication Laboratory (EFL) and Advanced Materials Characterization and Testing (AMCaT) facilities of University of California Davis for use of their machine equipment and confocal microscope facilities. The authors express their sincere thanks to Prof. Dr.-Ing. Jörg Seewig, Professor of the University of Kaiserslautern, Germany for his extended cooperation. Part of this work evolved in collaborative research within the International Research Training Group (IRTG) 2057 “Physical Modeling for Virtual

Manufacturing Systems and Processes." Thank you also to Jason Tsugawa for his help with the revision.

References

Asiltürk, İ., Neşeli, S., İnce, M.A., 2016. Optimisation of parameters affecting surface roughness of Co28Cr6Mo medical material during CNC lathe machining by using the Taguchi and RSM methods. Measurement 78, 120-128.

Asquith, D.T., Yerokhin, A.L., Yates, J.R., Matthews, A., 2007. The effect of combined shot-peening and PEO treatment on the corrosion performance of 2024 Al alloy. Thin Solid Films 516, 417-421.

Bigerelle, M., Mathia, T., Bouvier, S., 2012. The multi-scale roughness analyses and modeling of abrasion with the grit size effect on ground surfaces. Wear 286–287, 124-135.

Brown, C.A., Johnsen, W.A., Butland, R.M., Bryan, J., 1996. Scale-Sensitive Fractal Analysis of Turned Surfaces. CIRP Annals - Manufacturing Technology 45, 515-518.

Das, J., Linke, B., 2016. Effect of Manual Grinding Operations on Surface Integrity. Procedia CIRP 45, 95-98.

Davim, J.P., 2010. Surface integrity in machining. Springer.

De Chiffre, L., Lonardo, P., Trumpold, H., Lucca, D.A., Goch, G., Brown, C.A., Raja, J., Hansen, H.N., 2000. Quantitative Characterisation of Surface Texture. CIRP Annals - Manufacturing Technology 49, 635-652.

Ebbrell, S., Woolley, N.H., Tridimas, Y.D., Allanson, D.R., Rowe, W.B., 2000. The effects of cutting fluid application methods on the grinding process. International Journal of Machine Tools and Manufacture 40, 209-223.

Griffiths, B.J., 1993. Modelling Complex Force Systems, Part 1: The Cutting and Pad Forces in Deep Drilling. Journal of Engineering for Industry 115, 169-176.

Grzesik, W., 2016. Prediction of the Functional Performance of Machined Components Based on Surface Topography: State of the Art. Journal of Materials Engineering and Performance 25, 4460-4468.

Grzesik, W., Brol, S., 2003. Hybrid approach to surface roughness evaluation in multistage machining processes. Journal of Materials Processing Technology 134, 265-272.

Grzesik, W., Rech, J., Żak, K., 2015. Characterization of surface textures generated on hardened steel parts in high-precision machining operations. The International Journal of Advanced Manufacturing Technology 78, 2049-2056.

Grzesik, W., Żak, K., 2015. Possibilities of the Generation of Hardened Steel Parts With Defined Topographic Characteristics of the Machined Surfaces. Journal of Manufacturing Science and Engineering 137, 014502-014502.

Han, N., Mizan, M.F.R., Jahid, I.K., Ha, S.-D., 2016. Biofilm formation by Vibrio parahaemolyticus on food and food contact surfaces increases with rise in temperature. Food Control 70, 161-166.

Helmli, F., Pötsch, K., Repitsch, C., 2013. Choosing the Appropriate Parameter, Characterisation of Areal Surface Texture. Springer, pp. 155-177.

Hilbert, L.R., Bagge-Ravn, D., Kold, J., Gram, L., 2003. Influence of surface roughness of stainless steel on microbial adhesion and corrosion resistance. International Biodeterioration & Biodegradation 52, 175-185.

Javidi, A., Rieger, U., Eichlseder, W., 2008. The effect of machining on the surface integrity and fatigue life. International Journal of Fatigue 30, 2050-2055.

Jawahir, I.S., Brinksmeier, E., M'Saoubi, R., Aspinwall, D.K., Outeiro, J.C., Meyer, D., Umbrello, D., Jayal, A.D., 2011. Surface integrity in material removal processes: Recent advances. CIRP Annals - Manufacturing Technology 60, 603-626.
Kiyak, M., Çakır, O., 2007. Examination of machining parameters on surface roughness in EDM of tool steel. Journal of Materials Processing Technology 191, 141-144.
Krolczyk, G.M., Krolczyk, J.B., Maruda, R.W., Legutko, S., Tomaszewski, M., 2016. Metrological changes in surface morphology of high-strength steels in manufacturing processes. Measurement 88, 176-185.
Lavernhe, S., Quinsat, Y., Lartigue, C., Brown, C., 2014. Realistic simulation of surface defects in five-axis milling using the measured geometry of the tool. The International Journal of Advanced Manufacturing Technology 74, 393-401.
Leach, R., 2013. Characterisation of areal surface texture. Springer.
Linke, B., 2015. A review on properties of abrasives grits and grit selection. Int. J. of Abrasive Technology 7, 46-58.
Linke, B., Das, J., 2016. Aesthetics and Gloss of Ground Surfaces: A Review on Measurement and Generation. Journal of Manufacturing Science and Engineering 138, 064501-064501.
Lopes, R., Betrouni, N., 2009. Fractal and multifractal analysis: A review. Medical Image Analysis 13, 634-649.
Mandelbrot, B.B., 1989. Multifractal Measures, Especially for the Geophysicist, In: Scholz, C.H., Mandelbrot, B.B. (Eds.), Fractals in Geophysics. Birkhäuser Basel, Basel, pp. 5-42.
Matsumura, T., Sadakata, H., Makihata, H., Yoshino, M., 2013. Micro fabrication on cylinder surface for control of wettability. Journal of Manufacturing Processes 15, 8-13.
Metrology, M., 3D Surface Finish Roughness Texture Wear WYKO Veeco. CA Brown, PhD.
Nowicki, B., 1985. Multiparameter representation of surface roughness. Wear 102, 161-176.
Raymond, N., Hill, S., Soshi, M., 2016. Characterization of surface polishing with spindle mounted abrasive disk-type filament tool for manufacturing of machine tool sliding guideways. The International Journal of Advanced Manufacturing Technology, 1-14.
Seemikeri, C.Y., Brahmankar, P.K., Mahagaonkar, S.B., 2008. Investigations on surface integrity of AISI 1045 using LPB tool. Tribology International 41, 724-734.
Seyeux, A., Zanna, S., Allion, A., Marcus, P., 2015. The fate of the protective oxide film on stainless steel upon early stage growth of a biofilm. Corrosion Science 91, 352-356.
Simões, M., Simões, L.C., Vieira, M.J., 2010. A review of current and emergent biofilm control strategies. LWT - Food Science and Technology 43, 573-583.
Ţălu, Ş., Marković, Z., Stach, S., Todorović Marković, B., Ţălu, M., 2014. Multifractal characterization of single wall carbon nanotube thin films surface upon exposure to optical parametric oscillator laser irradiation. Applied Surface Science 289, 97-106.
Terry, A.J., Brown, C.A., 1997. A Comparison of Topographic Characterization Parameters in Grinding. CIRP Annals - Manufacturing Technology 46, 497-500.
Vulliez, M., Gleason, M.A., Souto-Lebel, A., Quinsat, Y., Lartigue, C., Kordell, S.P., Lemoine, A.C., Brown, C.A., 2014. Multi-scale Curvature Analysis and Correlations with the Fatigue Limit on Steel Surfaces after Milling. Procedia CIRP 13, 308-313.
Wang, Q., Liang, Z., Wang, X., Zhao, W., Wu, Y., Zhou, T., 2015. Fractal analysis of surface topography in ground monocrystal sapphire. Applied Surface Science 327, 182-189.
Wang, W.-z., Chen, H., Hu, Y.-z., Wang, H., 2006. Effect of surface roughness parameters on mixed lubrication characteristics. Tribology International 39, 522-527.
Whitehouse, D.J., 2011. Handbook of Surface and Nanometrology, Second ed. CRC Press, Taylor and Francis Group.

Zhang, L., Yue, G.H., 2016. Fractal Dimension Studies of the Brain Shape in Aging and Neurodegenerative Diseases, In: Di Ieva, A. (Ed.), The Fractal Geometry of the Brain. Springer New York, New York, NY, pp. 213-232.
Zhou, N., Peng, R.L., Pettersson, R., 2016. Surface integrity of 2304 duplex stainless steel after different grinding operations. Journal of Materials Processing Technology 229, 294-304.

Figure and Table Captions